Theoretical Rates for the Emission of Atomic Hydrogen from a Naphthalene Cation

T. Pino,*,† P. Parneix,† F. Calvo,‡ and Ph. Bréchignac†

Laboratoire de Photophysique Moléculaire, CNRS, Fédération de recherche Lumière Matière, Bât 210, Université Paris XI, F91405 Orsay Cedex, France, and Laboratoire de Chimie et Physique Quantiques, IRSAMC, Université Paul Sabatier, 118 Route de Narbonne, F31062 Toulouse Cedex, France

Received: December 11, 2006; In Final Form: March 19, 2007

The statistical phase space theory (PST) in its orbital transition state version has been used to calculate the dissociation rate associated with the loss of atomic hydrogen from a polycyclic aromatic hydrocarbon molecule. The PST model has been applied to the naphthalene cation with input data obtained exclusively from first-principle calculations using density functional theory. Without any fitting parameters, the calculated dissociation rates are found to agree well with available measurements. The effects of vibrational anharmonicities are investigated and are shown to lower the dissociation rates by a factor of about five.

I. Introduction

Polycyclic aromatic hydrocarbons (PAHs) are compounds of broad interest in fields ranging from combustion[1,2] and environmental studies[3] to interstellar carbon chemistry.[4–6] Currently, they are widely considered as prototypical molecules that are useful for better understanding the key processes involved in the cycle of carbon-based matter in space.[7] In particular, they may represent up to 20% of the cosmic carbon, and their presence is suggested by the ubiquitous aromatic infrared bands (AIBs) observed in emission at 3.3, 6.2, 7.7, 8.6, 11.3, and 12.7 μm.[7] The carriers of the AIBs were first tentatively identified as PAHs due to the strong similarities of infrared active vibrational band positions of this class of compounds.[8,9] The name of PAHs used in the astrophysical community actually refers to the many various possibilities of structures, charge states, and levels of hydrogenation that should occur in the different regions of the interstellar medium (ISM), as opposed to those usually studied in the laboratory having a well-defined chemical structure. Among the main reasons that historically led to the idea that PAHs might be present in the ISM, the mechanisms giving rise to the observed infrared emission are of primary importance.[7] Upon absorption of single photons from starlight, the AIBs carriers have to be small enough to experience sufficiently strong heating (up to about 500 K) to emit at such short wavelengths even in cold regions. Therefore, no steady-state thermal equilibrium within the radiation field is expected to be reached. Instead, due to the molecular size, multiple sequences of heating (via absorption) and cooling (via infrared emission, ionization, or fragmentation) are responsible for temperature spikes within which most of the infrared flux is radiated. The basic processes that need to be investigated are mainly those related to the interaction of PAHs with photons, which involve energy redistribution from the electronic excited states to the vibrational modes or to the competing dissociation channels, through a partial or complete internal conversion. Fragmentation is an important cooling channel because it will drive the size distribution of the astro-PAHs (i.e., those that are photostable); all molecules cannot survive when exposed to such a harsh radiation field.

This astrophysical issue motivated experimental studies in which fragmentation is triggered by ionization schemes,[10,11] either in ion traps[12–15] or using multiphoton processes.[16] With the advent of such experiments, it has become possible to determine the fragmentation channels, their appearance energy, and even the dissociation rates at specified excitation energies. Among the possible decay channels, these experimental studies have shown that the ejection of a single hydrogen atom is common to most PAHs and is even dominant for large size species, the second most frequently observed channel (loss of C_2H_2) being vanishingly small.[11] Considering the wide range of energies present in the interstellar medium, it would be useful to determine the dissociation rate at arbitrary excitations, at least up to 13.6 eV. The standard approach consists in combining theoretical models and experimental data.[17,18] The unimolecular dissociation of large molecules is described by statistical theories most often based on the Rice–Ramsperger–Kassel–Marcus (RRKM) or phase space theory (PST) frameworks. Because these models include many molecular data, simplified approaches using fitted parameters have been proposed.[17–19] Some important outcomes of these approaches are the dissociation energies and the activation entropy. The dehydrogenation channel was shown to be barrierless for cationic benzene[20,21] and naphthalene.[22] For larger molecules, a loose transition state was also reported by Lifshitz and co-workers.[17] Another outcome, namely the dissociation energies derived from fitting to experiment, is found to be systematically underestimated with respect to those predicted by quantum chemical calculations.[23,24] To reconcile the predictions of statistical theories with first principle data, it is advisable to develop a parameter-free approach. This is precisely what we aim for in the present paper, in relation with the ejection of one hydrogen atom from the naphthalene cation.

PST[25–27] was proven successful for describing the evaporation of weakly bound clusters for which the loose transition state hypothesis is satisfied.[18,19] In its orbiting transition state (OTS) version, the incorporation of energy and angular momenta constraints assuming a central interaction potential allows a

* To whom correspondence should be addressed. E-mail: thomas. pino@ppm.u-psud.fr.
† Laboratoire de Photophysique Moléculaire, CNRS, Laboratoire associé à l'Université ParisF/Sud.
‡ Laboratoire de Chimie et Physique Quantiques.

Emission of Atomic H from a Naphthalene Cation

J. Phys. Chem. A, Vol. 111, No. 20, 2007 **4457**

complete description of the dissociation process and provides thus some predictions for the rotational and translational energies released upon dissociation.[28-30] In particular, the dissociation rate and energy release are strongly influenced by the vibrational anharmonicities and the shape of the interaction potential between the fragments.[28-30] In the present work, we use a similar approach for modeling dehydrogenation from a PAH molecule. As will be seen below, the use of appropriate ab initio calculations provides all the necessary inputs for the PST model, making its predictions fully free from any fitting parameter. The naphthalene cation was chosen as a test molecule for which several experimental data and RRKM models are available in the literature.[10,12,13] Its small size also makes it tractable by standard quantum chemical methods. This paper is organized as follows. In section II, the PST approach is briefly described, and the results of the quantum chemical calculations are given in section III. The predicted rate constants are presented in section IV. We finally discuss in section V the limits of validity of our approach and provide rough error bars based on theoretical uncertainties.

II. PST Calculations

PST[25-27] has been used to calculate the absolute dissociation rate of PAH cations as a function of the internal energy. Along the dissociation coordinate, the loss of a hydrogen atom is known to be a barrierless process in the case of cationic benzene (refs 20 and 21), naphthalene (ref 22), and other positively charged PAHs.[17] Thus, for most cationic PAHs, the effective transition state of dissociation is located at the centrifugal barrier, and the orbiting transition state version of the PST formalism (PST/OTS) may be used to characterize the statistical properties, including the dissociation rate itself. The dissociation rate constant k_d can then be written as:

$$k_d(E) = \frac{K}{\Omega(E - E_r)} \int_0^{E-D_0} \Gamma(\epsilon_{tr}; E, J)\Omega'(E - D_0 - \epsilon_{tr})d\epsilon_{tr} \quad (1)$$

In this equation, the dissociation energy D_0 is equal to the difference of binding energies between the parent and product molecules, including the zero-point contributions. Ω and Ω' are the (quantum) vibrational densities of states (DOS) of the parent and product molecules, respectively. These statistical quantities have been calculated in the harmonic approximation by direct counting.[31] We denote by ϵ_{tr} the total kinetic energy released, corresponding to the sum of the translational and the rotational contributions. E_r is the initial rotational energy of the parent molecule. $\Gamma(\epsilon_{tr}; E, J)$ is the rotational density of states (RDOS). In the general case of a rotating parent molecule, it is given by

$$\Gamma(\epsilon_{tr}; E, J) = \int\int_{(S)} \gamma \, dJ_r \, dL \quad (2)$$

where L and J_r are the orbital and product angular momenta, respectively. The RDOS has been calculated by treating the product as a sphere with an effective rotational constant taken as the geometric average of the three rotational constants. Neglecting shape effects has been shown by Chesnavich and Bowers to produce only marginal errors in the rotational density.[32] In the sphere plus atom approximation, the number of available rotational states γ at the centrifugal barrier has a simple expression, namely $\gamma = 2J_r$. The integration domain (S) for the RDOS calculation is related to the energy and angular momentum conservation laws during the dissociation process. In particular, it depends on the height of the centrifugal barrier, which depends itself on the shape of the potential energy felt

by the dissociating hydrogen atom. We have considered the case where this potential is only governed by the long-range polarization interaction between the charge of the cation and the electric dipole induced on the dissociating hydrogen atom. We assume that this $1/r^4$ potential holds also in the vicinity of the centrifugal transition state. The validity of this approximation will be discussed further in the last section. Finally, in eq 1 the proportionality factor K is given by[19]

$$K = \frac{1}{h} \times \frac{1}{2J} \times g \quad (3)$$

in which h is the Planck constant, J is the initial angular momentum of the naphthalene cation, and g is a ratio of symmetry factors. While the PST framework explicitly includes the effects of an initially rotating parent (nonzero J) on all statistical properties, we have limited the present study to the cases where the naphthalene cation is nonrotating and J is equal to its mean thermal value $J_{th} \approx 65\hbar$ at 300 K for a relevant comparison with experimental data.

In this paper, we have used the statistical theory mainly for estimating the dissociation rate k_d associated with hydrogen emission from a PAH cation. However, it is also possible to calculate the probability distributions of the total kinetic energy released, ϵ_{tr}, and the angular momentum of the product molecule, J_r. These distributions and their average values will be used later to discuss the range of validity of our PST/OTS approach for the present problem.

All the ingredients required for applying the PST model have been obtained from density functional theory (DFT) calculations, for which a brief description will now be given.

III. DFT Calculations

Quantum chemical calculations were undertaken using the Gaussian 98 suite of programs.[33] The goal was to estimate the complete set of molecular data necessary for the fragmentation model. The ingredients list includes the binding energies of the parent and product molecules, their difference being the dissociation energy of the hydrogen atom. The optimized geometries are used to compute the rotational constants. The harmonic vibrational frequencies provide the vibrational densities of states, as well as the zero-point correction energies. Finally, the charge distribution affects the shape of the dissociation potential.

Several fragmentation channels have been considered in the present work, leading to the two isomers of $C_{10}H_7^+$, namely 1-naphthyl$^+$ and 2-naphthyl$^+$. Different low-energy states with different spin multiplicity had to be included in our calculations as well. While the parent cationic PAH has a doublet electronic ground state, the ground state of its fragment radicals may be either a triplet (for PAHs larger than cationic naphthalene) or a singlet in the case of $C_6H_5^+$.[20,23] In the case of naphthalene, the triplet and singlet states are found to be almost degenerate. Therefore, all the required properties were systematically calculated for all four different situations of products and electronic states at the same level of theory.

DFT was chosen for its ability to handle rather large molecules such as naphthalene. The effects of changing the functional and/or the basis sets were investigated following the conclusions of refs 22, 23, 34, and 35, also performing dedicated calculations. We first chose the B3LYP functional combined to the cc-pvdz Dunning-type basis sets as our main reference.[36] These calculations were compared to other data obtained using the B3PW91 functional, as well as the 6-31G* Pople-type basis sets.[37] We have not attempted to check convergence by

TABLE 1: Molecular Data for the $C_{10}H_8^+$ Naphthalene Cation and Its $C_{10}H_7^+$ Fragments in Their Triplet and Singlet Electronic States, Calculated Using the Basis Sets cc-pvdz and 6-31G* and the Two Functionals B3LYP and B3PW91[a]

molecule	molecular data	B3LYP/cc-pvdz	B3LYP/6-31G*	B3PW91/cc-pvdz	B3PW91/6-31G*
$C_{10}H_8^+$ (X^2A_u)	energy (Hartree)	−385.6310	−385.6136	−385.4833	−385.4618
	A (GHz)	3.126	3.135	3.138	3.145
	B (GHz)	1.215	1.219	1.221	1.223
	C (GHz)	0.875	0.878	0.879	0.881
	$\bar{\nu}_{ar}$ (cm^{-1})	1303	1309	1306	1311
	$\bar{\nu}_{geo}$ (cm^{-1})	1037	1040	1036	1039
fragment 1	ΔE_{elec} (eV)	5.13	5.15	5.13	5.13
	ΔE_{S-T} (eV)	0.09	0.11	0.09	0.12
	A (GHz)	3.290 (3.383)	3.299 (3.391)	3.302 (3.403)	3.310 (3.408)
	B (GHz)	1.211 (1.199)	1.214 (1.204)	1.215 (1.203)	1.218 (1.207)
	C (GHz)	0.885 (0.885)	0.888 (0.888)	0.888 (0.889)	0.890 (0.891)
	$\bar{\nu}_{ar}$ (cm^{-1})	1268 (1250)	1274 (1255)	1271 (1253)	1277 (1259)
	$\bar{\nu}_{geo}$ (cm^{-1})	1007 (974)	1011 (976)	1008 (976)	1011 (978)
fragment 2	ΔE_{elec} (eV)	5.20	5.21	5.20	5.21
	ΔE_{S-T} (eV)	0.07	0.09	0.08	0.10
	A (GHz)	3.147 (3.131)	3.158 (3.144)	3.157 (3.140)	3.167 (3.152)
	B (GHz)	1.257 (1.285)	1.261 (1.287)	1.262 (1.293)	1.265 (1.294)
	C (GHz)	0.898 (0.912)	0.901 (0.915)	0.901 (0.917)	0.904 (0.918)
	$\bar{\nu}_{ar}$ (cm^{-1})	1265 (1251)	1272 (1259)	1269 (1253)	1274 (1261)
	$\bar{\nu}_{geo}$ (cm^{-1})	1004 (983)	1008 (990)	1005 (981)	1008 (988)

[a] The values in the singlet electronic state a^1A' are given between parentheses. The absolute energies are reported only for the parent and relative energies (ΔE_{elec}) being given for the fragments. The energy gap ΔE_{S-T} between the a^1A' state and the X^3A'' triplet electronic states are given, the latter being considered as the electronic ground state according to the B3LYP results. Fragments 1 and 2 refer to the losses of hydrogen closest to and farthest from the center of mass, respectively. $\bar{\nu}_{ar}$ and $\bar{\nu}_{geo}$ are the arithmetic and geometric averages of the harmonic frequencies, respectively.

increasing the size of the basis set or to improve the predicted value by using another method such as coupled cluster, but instead we have tried to assess the reliability of such calculations by employing commonly used functionals and basis sets. Our long-term goal is to investigate larger PAH molecules for which such DFT calculations at these levels still stand as state-of-the-art. In addition, by combining two respected functionals and basis sets, the four PST results obtained provide a reasonable estimate of the variations of the molecular data associated with our theoretical calculation. The relevant data to be compared for the fragmentation model are reported in Table 1.

The absolute total energy is given for the parent molecule and relative values for the fragments. Although the absolute total energies obtained with B3PW91 are higher by about 4 eV, the relevant relative energies are found to be very similar to those obtained with the B3LYP functional. The $^3A''$ electronic state is confirmed to be the ground state of the $C_{10}H_7^+$ fragments, even including the zero-point energy, as already found in previous studies.[23,38] It should be noticed that the difference of ∼0.1 eV is somewhat comparable to the expected accuracy of such calculations. This small difference, specific to the naphthalene cation, implies that the singlet fragmentation channel should a priori be taken into account in the evaluation of the total fragmentation rate. However the $C_{10}H_7^+(a^1A')$ + $H(^2S)$ channel does not correlate to the $C_{10}H_8^+(X^2A_u)$ and cannot be included in our PST frame. To be actually competitive, this channel should involve a nonadiabatic process as is the case for cationic benzene.[20,21,39] However, the correlating A^2B_{1u} electronic state of $C_{10}H_8^+$ lies about 6000 cm^{-1} above the ground state,[40] and we do not expect any crossing point that would enhance the coupling. This problem was thoroughly analyzed by ab initio calculations in cationic benzene[20,21,39] in which the $C_6H_6^+(X^2A_2)$ ground state (given in the C_{2v} group of the $C_6H_5^+$ fragment) was seen to correlate to the $C_6H_5^+$-(X^3A_2) + $H(^2S)$ dissociation limit that lies nearly one eV above the lowest $C_6H_5^+(X^1A_1)$ + $H(^2S)$ channel. Therefore, a crossing point between the X^2A_2 and $^2A_1$ electronic states exists along the C−H coordinate of benzene$^+$. Such quantum chemical

investigations are out of scope of the present work. Moreover the singlet and triplet states are so close in energy that a multiconfiguration computation would be necessary to predict the potential curves with accuracy. Therefore only an upper limit of the possible contribution of this channel will be given in the next section.

The harmonic frequencies and the infrared spectra also agree with previous works obtained using smaller basis sets[41] or performed at a different level of theory.[42] On a side note, the differences in the vibrational spectra associated with the singlet and triplet states could provide information on the nature of the $C_{10}H_7^+$ fragments, the singlet state resembling that of the neutral fragment and the triplet state being closer to the cation ground state. For clarity, only the arithmetic and geometric averages have been reported in Table 1. The variations of these values upon changing the functional or the basis set provide an order of magnitude for the related error extracted from the dispersion of the values. As is usual for vibrational frequencies computed using such functionals,[43] a correction factor α = 0.96−0.98 is needed to reach a spectroscopic agreement with experimental positions of the IR active modes. Here we have chosen α = 0.97 for all frequencies. After this correction, and even though the different functionals yield similar values for a given basis set, the basis sets themselves seem to slightly affect the average frequencies for the two functionals. These differences should be hidden by the use of better functional and basis set-dependent correction factors. However, systematically different behaviors are found between the triplet and singlet states, the latter having lower frequencies.

For cationic naphthalene, the C−H binding energies can be evaluated, leading to values of about 4.8 ± 0.1 eV, in good agreement with previous calculations.[22,23] For the neutral molecule, comparable values are obtained with only a different ordering between the two fragments.[34,35,44] The energy difference is predicted to be 0.07 eV between the two channels. The 1-naphthyl$^+$ molecule is more stable and will be denoted as fragment 1. Such small differences imply that both isomers have to be included in the treatment of the H emission channel.
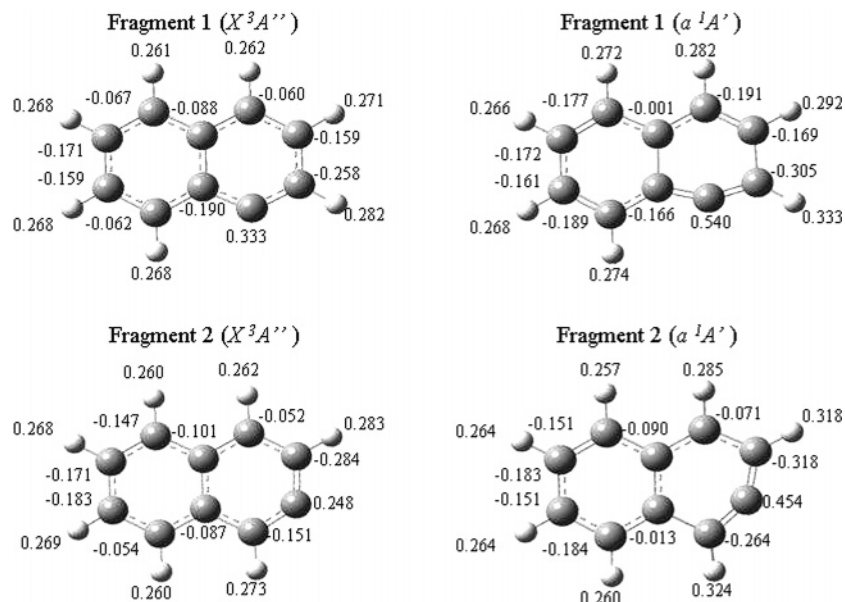
Emission of Atomic H from a Naphthalene Cation

J. Phys. Chem. A, Vol. 111, No. 20, 2007 **4459**

Figure 1. Optimized geometries of the $C_{10}H_7^+$ fragments obtained from DFT calculations at the B3LYP/cc-pvdz level for both the triplet and singlet electronic states. The NBO charge distributions are also indicated.

Turning now to the optimized geometries, they are similar and do not depend significantly on the functional or the basis set. In particular, the geometrically averaged rotational constants differ by less than 1%, which provides a further estimate of the typical error in the present calculation. The fragmentation products are found to rearrange by a small amount, mainly in the vicinity of the carbon atom involved in the C−H bond dissociation. Interestingly, only the singlet state of fragment 2 is found to be nonplanar.

The atomic charge distribution was calculated using the natural bond orbital (NBO) analysis.[45] No significant difference was found by changing the functional and/or the basis set, unlike with the Mulliken analysis. The main consequence of dehydrogenation of the naphthalene cation is that the charge of the carbon involved in the C−H bond breaking changes from a negative value of about −0.11(±0.05 depending on the carbon involved) to a positive value of about +0.29 (±0.04 depending on the isomer), while the charges of the two neighboring carbons are decreased by about −0.11. In Figure 1, the geometries and charge distributions are shown for $C_{10}H_7^+$ in the triplet and singlet states for the two different isomers.

IV. Results and Discussion

A. Results. In Table 1, we have summarized all the data needed in the PST calculation. The harmonic frequencies are used for the vibrational densities of states of both the parent and product molecules. Because the VDOSs exponentially depend on the frequencies, the scaling factor α can critically affect the dissociation rates. In Figure 2a, we have represented the variations of the absolute dissociation rate with increasing excitation energy for the three typical (and reasonable) values $\alpha = 0.96$, 0.97, and 0.98. Here, only the dissociation leading to fragment 1 in its lowest triplet electronic state was considered, the parent being nonrotating. A variation within a factor of 2 is found as α increases from 0.96 to 0.98. Generally speaking, the rate decreases with α, which is consistent with the expected scaling of the dissociation rate with the average vibrational frequencies. In Figure 2b, the influence of D_0 on the rate constant has also been explored. As is commonly accepted, these dissociation energies are typically accurate within about 0.1 eV. We have thus repeated the calculation of k_d by changing the
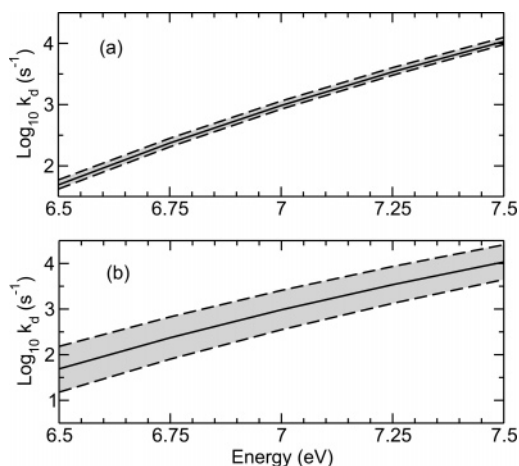

Figure 2. H loss dissociation rates for fragment 1 in its triplet state channel as a function of internal energy at $J = 0$. (a) Rates obtained for scaling factors of 0.97 (solid line), 0.96 (lower dashed line), and 0.98 (upper dashed line). (b) Rates obtained for dissociation energies of 4.79 (solid line), 4.89 (lower dashed line), and 4.69 eV (upper dashed line).

dissociation energy by ±0.1 eV. As D_0 varies by 0.2 eV, the rate changes by a factor of about 8, k_d being obviously higher for lower dissociation energies.

As was previously discussed, two products of the naphthalene cation upon hydrogen emission are found, and for both of them the degeneracy factor g (see eq 3), corresponding here to the number of equivalent H, is equal to 4. To show the importance of considering all the channels, the individual dissociation rates have been calculated at the two internal energies corresponding to the experimental conditions reported in the literature[11,13] and in an initial rotational state J_{th}. These energies and the results of these calculations are given in Table 2. It should be first noted that all individual rates vary by less than a factor 2. Therefore, the contributions of the two channels are comparable. Their precise, individual evaluations should be necessary for larger cationic PAHs because there are more nonequivalent hydrogens and the dissociation rate depends critically on the binding energy. Such analysis would open the possibility to

TABLE 2: Calculated Dissociation Rates (in s^{-1}) for the Two Different Isomers in the Two Different Electronic States for the Product Cation C$_{10}$H$_7^+$, as Well as the (Total) Predicted Dissociation Rate for the Dehydrogenation of C$_{10}$H$_8^{+a}$

energy (eV)	T (frag 1)	T (frag 2)	total k_d	exp	S (frag 1)	S (frag 2)
7.1	1434	844	2278	2230	2840	1175
(7.13)	(139)	(77)	(216)	(620)[13]	(251)	(100)
7.4	6176	3812	9988	10000[11]	12962	5561

^{a} The excess energies are chosen close to the experimental estimates and the initial J is taken to be equal to its average thermal value at 300 K $J_{th} \approx 65\hbar$. Available experimental rates are also reported for comparison.[11,13] The values between parentheses correspond to per-deuterated species. S and T refer to the singlet and triplet electronic states of the fragments, respectively, and the related singlet states values are given to evaluate the upper limit of the contribution of this channel (see text for details).
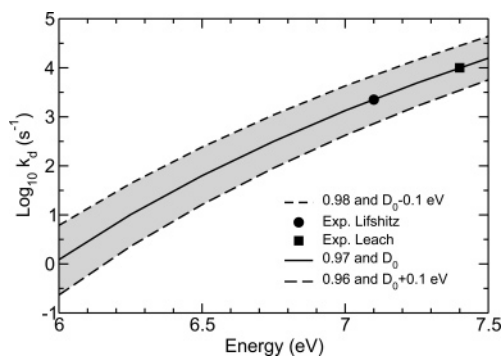

Figure 3. Total dehydrogenation rate for the naphthalene cation as a function of internal energy at $J = J_{th}$. The solid line corresponds to the calculation with $\alpha = 0.97$ and the D_0 values directly obtained from DFT calculations. The two extreme predicted cases based on the uncertainties of the quantum chemical calculations input values are shown. Experimental values are also shown.[11,13]

check if an average binding energy could be used instead of individual energies, owing to the dispersion of the calculated values.

In Figure 3, we have represented the variations of the total dissociation rate k_d with increasing excess energy, at $J = J_{th}$. Based on the theoretical uncertainties inferred in the previous section, two other calculations have been carried out by either increasing D_0 while decreasing α, or by decreasing D_0 while increasing α. Such changes, which stand as two extreme cases, provide approximate orders of magnitude for the theoretical uncertainties of the present DFT-based calculations. The two independent experimental data available for this system[11,13] have also been reported in Figure 3. From a general point of view, our PST approach predicts absolute dissociation rates in good agreement with measurements. In particular, the variations with energy are well reproduced.

In a previous work,[46] some of us proposed a theoretical model for evaluating the influence of anharmonicities of the potential energy surface on the quantum vibrational densities of states as a function of internal vibrational energy. It must be emphasized that this dependence is not recovered by the scaling factor of the predicted harmonic frequencies, which provides a correction only in the vicinity of the vibrational ground state. This model was applied to the case of the neutral naphthalene molecule in ref 47. In the present work, we performed a similar calculation for ionic naphthalene. We assumed that the same energy dependence of the anharmonicity factor can be taken for C$_{10}$H$_8^+$ and C$_{10}$H$_7^+$. The effects of vibrational anharmonicities are shown in Figure 4 in which k_d, obtained using either
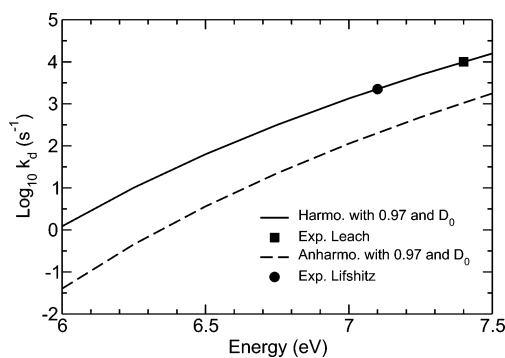

Figure 4. Total dehydrogenation rate for the naphthalene cation as a function of internal energy, with or without anharmonicity corrections, at $J = J_{th}$. The experimental values are also reported.[11,13]

harmonic or anharmonic densities, is plotted against excess energy for $J = J_{th}$. In the experimentally relevant energy range (for internal energies close to 7 eV), the dissociation rate decreases by a factor 5 when using anharmonic densities of states. Such a decrease is mainly due to the increase of the density of states in the parent, while it increases more slowly in the fragment due to fewer degrees of freedom. In addition, the DOS of the fragment remains close to the harmonic value because of its much lower internal energy. This effect appears to be of comparable importance to the sensitivity of the rates to the binding energies and should therefore not be neglected.

The PST/OTS frame of the present dissociation model does not account for nonadiabatic channels, such as the one leading to the singlet electronic state of the ionic fragment. In the naphthalene cation, this state is found to be quasi-degenerate with the triplet electronic ground state and might contribute to the overall fragmentation rate. However, we have only provided an attempt to quantify an upper limit for this contribution. As stated previously, we do not expect any crossing point or potential barrier along this reaction path. Therefore, in the spirit of the modified PST approach used by Gridelet et al.[39] the effective interaction potential of the C$_{10}$H$_7^+$(X^{1}A$'$) + H(^{2}S) channel was considered simply as having the same shape as that leading to the C$_{10}$H$_7^+$(X^{3}A$''$) + H(^{2}S) channel. This implies that the nonadiabatic dynamics along this path is very efficient and does not hinder dissociation, and that the centrifugal barrier lies at distances between fragments that are large enough. Using the molecular data taken from the DFT calculations and assuming that the long-range interaction between the fragments is of the charge/induced dipole type, we have estimated the dissociation rates for two isomers of the naphthalene cation into the two electronic states of the product. The results are reported in Table 2. For each isomer, this upper limit appears to be an upper bound yet similar to the value of the constant to the triplet state. Because the triplet state is lower in energy, this result seems surprising. However, the lower frequencies of the isomers in the singlet state tend to increase the vibrational densities, an entropic effect which more than compensates for the loss in binding energy. Therefore, including the singlet channel leads to an increase in the total predicted fragmentation rate by a factor of 2 at maximum.

B. Discussion. *1. Comparison with Experimental Data.* The values obtained in this work are in rather good agreement with available experimental data. Unfortunately, no error bars were given for these difficult measurements. In the work by Jochims et al.,[11] the appearance energy was considered as corresponding to a rate of 10^4 s^{-1} from previous measurements of hydrogen emission from the benzene molecule.[49,50] It is unclear whether such experiments should yield strictly similar measurable

Emission of Atomic H from a Naphthalene Cation

J. Phys. Chem. A, Vol. 111, No. 20, 2007 **4461**

kinetics. In the work by the Lifshitz group, the value of 4×10^4 s^{-1} at the approximate energy of 7 eV was initially reported,[12] but was contradicted by their most recent measurements of about 2×10^4 s^{-1} (ref 13), which we take as a more reliable reference in Table 2. We can thus consider that the predictions of our model fall within the experimental range up to a factor of 5. In Table 2, the rate constant calculated for perdeuterated species has also been reported. Again, the agreement with experimental data is very satisfactory.

Because of a large kinetic shift (i.e., the excess energy required to induce detectable dissociation),[18] the binding energies have to be extracted from statistical models. In most experimental studies, the models used are Rice−Ramsperger−Kassel (RRK), RRKM, or variational transition state theory.[11,13,50] In general, significant discrepancies are found between the fitted value for D_0 and quantum chemical calculations. Such differences imply that the energy dependence of the dissociation rate might not be well reproduced using the fitted data. On the other hand the present, more sophisticated, statistical PST/OTS model combined with quantum chemical calculations reconciles experimental and first-principles approaches without introducing any fitting procedure. This should open the way for predictive calculations on larger PAHs molecules.

2. Limitations of the PST Model. The PST results discussed in the previous section have been obtained by assuming that the hydrogen atom dissociating from the naphthalene cation feels a simple radial potential $V(r)$ with the form of a point charge polarization interaction $V(r) \sim C/r^4$. In using this form, r measures the distance between the hydrogen atom and the center of mass of the parent molecule $C_{10}H_8^+$. This potential has been previously used by Klippenstein et al.[50] for the analysis of the H loss channel of $C_6H_6^+$. However, more recently it was shown to be unsuited in the case of the dehydrogenation from this cation.[20,21] A significant approximation in the expression of the dissociation potential is the pointlike character of the fixed charge, which in turn allows the use of the OTS framework. As the size of the PAH molecule increases, the charge distribution is expected to become less localized[51] and the C/r^4 form should be less accurate. In general, the approximation will be valid if the centrifugal barrier is located at distances that are long enough.

We have attempted to quantify the validity of the pointlike approximation for this long-range dissociation potential by comparing the pair potential in which the charge +1 is located at the center of mass of the fragment with the curve obtained using the NBO distribution of partial charges in the ground-state configuration of the triplet state (fragment 1, see Figure 1). The two potentials, represented in Figure 5, become similar within less than 0.01 eV when the distance between the dissociating hydrogen atom and the closest carbon atom exceeds about 2 Å. However, the validity of the pure polarization interaction also implies that there are no remains of chemical bonding as the hydrogen atoms crosses the centrifugal barrier. The extent of chemical bonding as a function of the C−H distance has been studied by Jolibois et al.[22] using DFT calculations. These authors have shown that the C−H interaction decreases very rapidly for increasing distances and is very small beyond $r_{CH} \sim 3$ Å. However, Klippenstein[20] has shown that even at $r_{CH} \sim 4$ Å, ab initio calculations predict that chemical bonding is still stronger than polarization forces, the interaction potential between cationic benzene and hydrogen being correctly described by this potential only above $r_{CH} \approx 7-8$ Å. For the present case of $C_{10}H_8^+$, the simple form $1/r^4$ should thus underestimate the real interaction potential but may be consid-
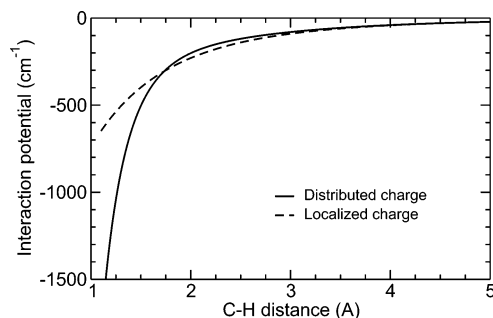

Figure 5. Dissociation potential of the hydrogen atom emitted from $C_{10}H_8^+$ for fragment 1 in the triplet state, using either a point-like charge located at the center of mass (dashed line) or the more realistic charge distribution obtained from the NBO analysis (solid line). The potentials resulting from the charge distribution of fragment 2 and in the singlet states are similar to that presented.
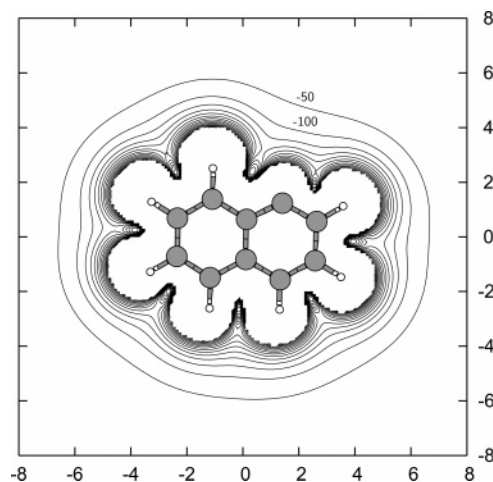

Figure 6. Two-dimensional contour map of the interaction potential felt by the hydrogen atom emitted from $C_{10}H_8^+$ and the "ionic core" fragment 1 in its triplet state in the aromatic plane, using its charge distribution obtained from the NBO analysis. The contour increment is 50 cm^{-1}, and the H atom-center of mass distance unit is in angstrom. Note the anisotropic shape of the potential for center of mass distances below ∼5 Å. Above this value, the potential converges to the simple central Langevin model interaction (see Figure 5) and becomes almost isotropic.

ered as one model potential in the long-range region of the potential energy surface.

Recently, the applicability of an PST/OTS approach for the H emission from the benzene cation and smaller hydrocarbons has been questioned by Gridelet et al. [refs 21 and 39]. The main conclusions pointed to the failure of the simple central polarization interaction potential but not only due its underestimate character. The introduction of the rotational contribution through the RDOS of the fragment indicates that the translational and rotational motions are separable during dissociation.[21] The central potential assumption is crucial in the PST/OTS framework, and the interaction will indeed be isotropic only if the centrifugal barrier itself is located at a long enough distance $r^\dagger$. To check for the isotropic character of the simple interaction used here, a contour plot of the long-range dissociation potential using the NBO charge distribution has been calculated and is shown in Figure 6. It appears that for $r \geq 5$ Å, the anisotropic character of the potential energy surface clearly diminishes thus providing an estimate for the distance where the interaction becomes radial. Therefore, we considered this potential as a model potential that should be satisfactorily valid in the limit of applicability of the PST/OTS formalism.

We have thus tried to estimate the location of the centrifugal barrier in our calculation for excess energies close to experimental values. The average angular momentum $\langle J_r \rangle$ of the fragment has been calculated for energies between 5.5 and 7.5 eV at every 0.5 eV (data not shown here). In this range, the angular momentum increases from 15 to $18\hbar$. When the initial angular momentum is very small, the orbital momentum ℓ compensates for the product angular momentum, hence $\ell \simeq \langle J_r \rangle \simeq 15-18\hbar$. These values correspond to centrifugal barriers located at distances $r^\dagger \simeq 4.5-3.5$ Å in the case of fragment 1. For fragment 2, the situation is less favorable due to the longer equilibrium distance between the carbon atom and the center of mass. $r^\dagger$ is then reduced by about 0.9 Å with respect to fragment 1. A shift of $+0.15$ Å is found for the perdeuterated species for both fragments. From these results, the centrifugal barrier appears to be located at distances where the $1/r^4$ radial potential clearly underestimates the interaction energy because chemical bonding dominates, and this model potential is therefore not appropriate. In addition, it is clear that at such small distances steric effects have to be included, as revealed by the contour plot of the interfragment potential in Figure 6. However, at the present stage the description can be considered as satisfactory for fragment 1 when the excitation energy does not exceed about 7 eV. In fragment 2, the centrifugal barrier is not correctly estimated due to the enhanced geometric extension, hence the rotational distribution and the kinetic energy released will be even more approximate. However, the kinetic energy release is rather small (0.1−0.2 eV) compared to the vibrational energy stored in the naphthyl fragment (∼2 eV). Therefore, a better potential should lead to small variations in the predicted dissociation rates, comparable to those introduced by the dispersion of the quantum chemical calculations. The stronger interaction should move the centrifugal barrier toward longer $r^\dagger$ distances and more isotropic regions, even though we do not expect significant changes in the calculated dissociation rates.

In addition to the necessary isotropic character of the potential energy surface, the relevance of the PST/OTS approach for hydrogen emission from the benzene cation and smaller hydrocarbons has been discussed in concern with an adiabaticity criterion by Gridelet and co-workers[21] and by Troe et al.[52] The evaluation of this constraint was proposed through the Massey parameter, which assesses the adiabaticity of the channel. This quantity was built considering that the translational motion must be much slower that the rotational motion of the ionic fragment.[21] Its evaluation leads to a dissociation with a maximum of translational kinetic energy release of about 10^{-3} eV.[21] This value should be of the same order for the H emission from cationic naphthalene and is well below the present typical value of about 0.1 eV at the experimental excitation energies (Table 2). Even when the excess energy is about 1 eV above D_0, the centrifugal barrier is found at $r^\dagger \simeq 5$ Å, which is large enough to satisfy the isotropy criterion, with the H translational kinetic energy being then about 0.05 eV. However, as discussed by Troe et al.,[52] if the potential energy surface is isotropic, a very small Massey parameter would correspond to the "sudden" limit and the dissociation may then be treated by phase space theory. This limit corresponds to a fast translational motion compared to the rotational one, and it is equivalent here to a translational kinetic energy release much higher than 10^{-3} eV. Therefore, a detailed analysis of the kinetic energy redistribution by using a better interfragment potential is necessary to investigate the role of the nonadiabatic effects.

V. Conclusions and Outlook

PST has been applied to the statistical dehydrogenation of the naphthalene cation. First-principle inputs from DFT calculations have been used in the model to calculate the dissociation rates without employing any fitting procedure. By choosing two popular functionals and two commonly used basis sets, we have also provided typical uncertainties in our predictions. Two isomers have been considered in the calculation to describe the fragmentation products. A simple polarization interaction with C/r^4 form was assumed for the long-range potential felt by the dissociating hydrogen atom.

A good agreement between the calculated dissociation rates and the available measurements has generally been obtained. Comparing the theoretical values to experimental data, our results suggest that the two isomers of the $C_{10}H_7^+$ fragment both contribute to the overall rate on a comparable footing. Because the experimental data are located in a rather narrow range of excitation energy, it would be highly desirable to have extra measurements at smaller internal energy to assess our theoretical predictions in a wider energy range.

By analyzing the location of the centrifugal barrier, we have estimated that the present PST/OTS model for the radial potential should be valid for excitation energies up to approximately 6.5−7 eV (i.e., when the resulting centrifugal barrier is located in the region where the potential between the ionic fragment and the emitted hydrogen is radial) and for emission velocities that are high enough so that the rotation of the main fragment can be neglected. Such considerations place the available measurements in the upper part of this validity range. In most cases, and if the initial angular momentum is no longer small, the radial potential should be modified to account for the residual chemical bonding at shorter C−H distances where pure polarization underestimates the interaction in a way similar to the approach used by Harding et al.[53] Such a quantum chemical potential should become close to the $1/r^4$ polarization interaction used here at long distances and be sensitive to the spatial extension of the ionic fragment at moderate distances. This would allow a precise evaluation of the energy region where anisotropic effects would prevail and make the present PST/OTS approach fail in describing accurately the statistics of dissociation.

Interestingly, the limitations of our OTS/PST model are in concordance with the objectives of using this model in the astrophysical context. Only molecules with a low dissociation rate in the energy range of interest are relevant because they are able to survive in the ISM. However, our aim is to describe properly the dissociation over a broad energy range. Therefore, some improvements of the present approach are necessary. These improvements include using a different form for the dissociation potential, treating the fragments as symmetric tops rather than spherical tops. Moreover, because of the light mass of the hydrogen atom, it would be useful to account for the possible tunneling effects through the centrifugal barrier. These improvements will allow detailed investigations of the kinetic energy release and its distribution that needs to be performed to check whether an PST/OTS approach can be used or if nonadiabatic dynamics could dominate. Even without such refinements, the present PST approach seems very promising for obtaining a quantitative picture of statistical dehydrogenation of PAH cations for any molecule that can be handled by standard quantum chemical calculations.

References and Notes

(1) Fialkov, A. B.; Dennebaum, J.; Homann, K. H. *Combust. Flame* **2001**, *125*, 763 and references therein.

(2) Frenklach, M. *Phys. Chem. Chem. Phys.* **2002**, *4*, 2028 and references therein.

(3) Keith, L. H.; Telliard, W. A. *Environ. Sci. Technol.* **1979**, *13*, 416.

(4) Duley, W. W. *Faraday Discuss.* **2006**, *133*, 415.

(5) Ehrenfreund, P.; Sephton, M. A. *Faraday Discuss.* **2006**, *133*, 277.

(6) Zubko, V.; Dwek, E.; Arendt, R. G. *Astrophys. J., Suppl. Series* **2004**, *152*, 211.

(7) Puget, J. L.; Léger, A. V. *Ann. Rev. Astron. Astrophys.* **1989**, *27*, 161.

(8) Léger, A.; Puget, J. L. *Astron. Astrophys.* **1984**, *137*, L5.

(9) Allamandolla, L. J.; Tielens, A. G. G. M.; Barker, J. R. *Astrophys. J.* **1985**, *290*, L25.

(10) Jochims, H. W.; Rasekh, H.; Rühl, E.; Baumgärtel, H.; Leach, S. *Chem. Phys.* **1992**, *168*, 159.

(11) Jochims, H. W.; Baumgärtel, H.; Leach, S. *Astrophys. J.* **1999**, *512*, 500.

(12) Ho, Y.-P.; Dunbar, R. C.; Lifshitz, C. *J. Am. Chem. Soc.* **1995**, *117*, 6504.

(13) Cui, W.; Hadas, B.; Cao, B.; Lifshitz, C. *J. Phys. Chem. A* **2000**, *104*, 6339.

(14) Boissel, P.; Parseval, P.; Marty, P.; Lefèvre, G. *J. Chem. Phys.* **1997**, *106*, 4973.

(15) Banisaukas, J.; Szczepanski, J.; Eyler, J.; Vala, M. *J. Phys. Chem. A* **2004**, *108*, 3723.

(16) Nguyen Thi, V.-O.; Desesquelles, P.; Douin, S.; Bréchignac, P. *J. Phys. Chem. A* **2006**, *110*, 5592.

(17) Lifshitz, C. *Int. Rev. Phys. Chem.* **1997**, *16*, 113.

(18) Lifshitz, C. *Eur. J. Mass Spectrom.* **2002**, *8*, 85.

(19) Jarrold, M. F. In *Clusters of Atoms and Molecules I*; Haberland, H., Ed.; Springer-Verlag: Berlin, 1991.

(20) Klippenstein, S. J. *Int. J. Mass. Spectrom.* **1997**, *167*, 235.

(21) Gridelet, E.; Lorquet, A. J.; Locht, R.; Lorquet, J. C.; Leyh, B. *J. Phys. Chem. A* **2006**, *110*, 8519.

(22) Jolibois, F.; Klotz, A.; Gadéa, F.-X.; Joblin, C. *Astron. Astrophys.* **2005**, *444*, 629.

(23) Bauschlicher, C. W., Jr.; Langhoff, S. R. *Mol. Phys.* **1999**, *96*, 471.

(24) Fujiwara, K.; Harada, A.; Aihara, J. *J. Mass Spectrom.* **1996**, *31*, 1216.

(25) Pechukas, P.; Light, J. C. *J. Chem. Phys.* **1965**, *42*, 3281.

(26) Klots, C. E. *J. Phys. Chem.* **1971**, *75*, 1526.

(27) Chesnavich, W. J.; Bowers, M. T. *J. Am. Chem. Soc.* **1976**, *98*, 8301.

(28) Calvo, F.; Parneix, P. *J. Chem. Phys.* **2003**, *119*, 256.

(29) Parneix, P.; Calvo, F. *J. Chem. Phys.* **2003**, *119*, 9469.

(30) Calvo, F.; Parneix, P. *J. Chem. Phys.* **2004**, *120*, 2780.

(31) Stein, S.; Rabinovitch, B. S. *J. Chem. Phys.* **1973**, *58*, 2438.

(32) Chesnavich, W. J.; Bowers, M. T. *J. Chem. Phys.* **1977**, *66*, 2306.

(33) Frisch, M. J.; Trucks, G. W.; Schlegel, H. B.; Scuseria, G. E.; Robb, M. A.; Cheeseman, J. R.; Zakrzewski, V. G.; Montgomery, J. A., Jr.; Stratmann, R. E.; Burant, J. C.; Dapprich, S.; Millam, J. M.; Daniels, A. D.; Kudin, K. N.; Strain, M. C.; Farkas, O.; Tomasi, J.; Barone, V.; Cossi, M.; Cammi, R.; Mennucci, B.; Pomelli, C.; Adamo, C.; Clifford, S.; Ochterski, J.; Petersson, G. A.; Ayala, P. Y.; Cui, Q.; Morokuma, K.; Malick, D. K.; Rabuck, A. D.; Raghavachari, K.; Foresman, J. B.; Cioslowski, J.; Ortiz, J. V.; Stefanov, B. B.; Liu, G.; Liashenko, A.; Piskorz, P.; Komaromi, I.; Gomperts, R.; Martin, R. L.; Fox, D. J.; Keith, T.; Al-Laham, M. A.; Peng, C. Y.; Nanayakkara, A.; Gonzalez, C.; Challacombe, M.; Gill, P. M. W.; Johnson, B. G.; Chen, W.; Wong, M. W.; Andres, J. L.; Head-Gordon, M.; Replogle, E. S.; Pople, J. A. *Gaussian 98*, revision A.9; Gaussian, Inc.: Pittsburgh, PA, 1998.

(34) Barckholtz, C.; Barckholtz, T. A.; Hadad, C. M. *J. Am. Chem. Soc.* **1999**, *121*, 491.

(35) Cioslowski, J.; Liu, G.; Martinov, M.; Piskorz, P.; Moncrieff, D. *J. Am. Chem. Soc.* **1996**, *118*, 5261.

(36) Dunning, J. T. H. *J. Chem. Phys.* **1993**, *90*, 1358.

(37) Ditchfield, R.; Hehre, W. J.; Pople, J. A. *J. Chem. Phys.* **1971**, *54*, 724.

(38) Du, P.; Salama, F.; Loew, G. H. *Chem. Phys.* **1993**, *173*, 421.

(39) Gridelet, E.; Lorquet, J. C.; Leyh, B. *J. Chem. Phys.* **2005**, *122*, 094106.

(40) Negri, F.; Zgierski, M. Z. *J. Chem. Phys.* **1994**, *100*, 1387.

(41) Bauschlicher, C. W., Jr.; Langhoff, S. R. *Chem. Phys.* **1998**, *234*, 79.

(42) Pauzat, F.; Talbi, D.; Ellinger, Y. *Astron. Astrophys.* **1995**, *293*, 263.

(43) Langhoff, S. R. *J. Phys. Chem.* **1996**, *100*, 2819.

(44) Berkowitz, J.; Ellison, G. B.; Guttman, D. *J. Phys. Chem.* **1994**, *98*, 2744.

(45) Reed, A. E.; Curtiss, L. A.; Weinholt, F. *Chem. Rev.* **1988**, *88*, 899.

(46) Parneix, P.; Nguyen-Thi, V.-O.; Bréchignac, Ph. *Chem. Phys. Lett.* **2002**, *357*, 78.

(47) Nguyen-Thi, V.-O.; Parneix, P.; Bréchignac, P. *Phys. Chem. Chem. Phys.* **2005**, *7*, 1779.

(48) Weerasinghe, S.; Amar, F. G. *J. Chem. Phys.* **1993**, *98*, 4967.

(49) Kühlewind, H.; Kiermeier, A.; Neusser, H. J.; Schlag, E. W. *J. Chem. Phys.* **1987**, *87*, 6488.

(50) Klippenstein, S. J.; Faulk, J. D.; Dunbar, R. C. *J. Chem. Phys.* **1993**, *98*, 243.

(51) Rapacioli, M.; Calvo, F.; Joblin, C.; Spiegelman, F.; Wales, D. J. *J. Phys. Chem. A* **2005**, *109*, 2487.

(52) Troe, J.; Ushakov, V. G.; Viggiano, A. A. *Z. Phys. Chem. A* **2005**, *219*, 715.

(53) Harding, J. B.; Georgievskii, Y.; Klippenstein, S. J. *J. Phys. Chem. A* **2005**, *109*, 4646.